



Feasibility study of measuring instantaneous angular speed of helical gears with magnetoresistive sensors

Yanik Koch¹ · G. Martin² · E. Kirchner³ · D. Quirnheim Pais⁴ · R. Slatter⁵

Received: 10 March 2022 / Accepted: 20 June 2022 / Published online: 12 July 2022
© The Author(s) 2022

Abstract

The digitalization of industrial processes with e.g. the goal to increase the availability of production processes in general and to support the individualization of many products in particular leads to an increasing demand in sensor data. The state of the art for condition monitoring of involute gear trains is the measurement of structure-borne vibration with acceleration sensors. New approaches, such as measuring the instantaneous angular speed (IAS), are gaining in popularity. Machine manufacturers usually wish to use existing sensors or measurement points, where little or no effort is needed to implement the sensor concept. Magnetoresistive (MR) sensors fulfil this complex set of requirements to a high degree: They are comparatively easy to integrate, can be added as an optional component and provide sufficient accuracy. The authors have developed different sensor concepts using MR sensors for measuring IAS in a 1-stage helical gear box. Multiple tests with artificial tooth flank damages have been carried out to evaluate the damage detection potential of the sensor concepts. Finally, a spectrum analysis of the first gear mesh frequency and surrounding sidebands demonstrates the capability for detecting tooth flank damage with different MR sensor concepts.

Machbarkeitsstudie zur Messung der Momentanen Winkelgeschwindigkeit mit Magnetoresistiven Sensoren in Schrägverzahnten Stirnradgetrieben

Zusammenfassung

Die Digitalisierung von industriellen Prozessen mit dem Ziel, die Verfügbarkeit von Produktionsprozessen im Allgemeinen zu erhöhen und die Individualisierung vieler Produkte zu unterstützen, führt zu einem steigenden Bedarf an Sensordaten. Stand der Technik zur Zustandsüberwachung von Evolventengetrieben ist die Messung von Körperschall mit Beschleunigungssensoren. Neue Ansätze, wie z.B. die Messung der momentanen Winkelgeschwindigkeit (IAS), gewinnen an Bedeutung. Maschinenhersteller wollen in der Regel vorhandene Sensoren oder Messstellen nutzen, bei denen ein geringer oder gar kein Aufwand zur Umsetzung des Sensorkonzepts erforderlich ist. Magnetoresistive (MR) Sensoren erfüllen diesen komplexen Anforderungen in hohem Maße: Sie sind vergleichsweise einfach zu integrieren, können optional hinzugefügt werden und bieten eine ausreichende Genauigkeit.

Die Autoren haben verschiedene Sensorkonzepte mit MR-Sensoren zur Messung der momentanen Winkelgeschwindigkeit in einem einstufigen Stirnradgetriebe entwickelt. Es wurden mehrere Tests mit künstlich eingebrachten Zahnflankenschäden durchgeführt, um das Potenzial der Sensorkonzepte Schäden zu erkennen zu bewerten. Die Auswertung findet mit einer Spektrumsanalyse der ersten Zahneingriffsfrequenz und der umliegenden Seitenbänder statt.

✉ Yanik Koch
Yanik.koch@tu-darmstadt.de

¹ Produktentwicklung und Maschinenelemente, Technische Universität Darmstadt, Darmstadt, Germany

² HCP Sense GmbH, Technische Universität Darmstadt, Darmstadt, Germany

³ Technische Universität Darmstadt, Darmstadt, Germany

⁴ Sensitec GmbH, Wetzlar, Germany

⁵ ITK Dr. Kassen GmbH, Lahnau, Germany

1 Introduction

Several current mega-trends in engineering accelerate the development of new sensor concepts. The digitalization of industrial processes with e.g. the goal to increase the availability of production processes in general and to support the individualization of many products in particular [1], requires additional sensor data. Independent of the maturity level of the system under consideration, mechatronic, smart and intelligent systems all require sensor data for control, reliability, interoperability and autonomy. Intelligent sensors, which can monitor the condition of critical machine components, are an “enabling technology” for availability-oriented Product-Service-Systems. They provide information that can be offered as a service. Pay-per-Use business models are now appearing in the machine tool, printing machine and packaging machine industries, which rely on accurate information about machine condition, in order to guarantee an agreed level of machine availability [2, 3]. Hence, many different approaches are applied to gather information about the condition of machine elements, such as gears, rolling bearings or ball screws.

An established model to support condition monitoring of involute gear trains is based on an order analysis of the system vibrations with one or three-dimensional accelerometers and an associated method is to measure acoustic emissions. However, new approaches such as the measurement of instantaneous angular speed (IAS) are gaining in popularity [4, 5]. This measuring technique makes special demands of the sensors used. They must not only be small, precise and robust, but must also have a high bandwidth and a low power requirement. In addition to this, the manufacturer of the machine often wishes to use existing sensors or measurement points to realize this additional functionality, that is, they wish to avoid the implementation of additional sensors if possible. Until now optical encoders have typically been used for measuring IAS. However, these encoders are attached to a shaft and therefore directly influence the power transmitting elements.

Therefore, this paper presents sensor concepts for measuring IAS and the detection of gear flank damage. The sensor concepts have little to no influence on and do not alter the power transmitting elements. Of particular interest is the use of a gear wheel as measuring scale. Finally, their ability to detect artificial tooth flank damage is investigated to evaluate the possibilities of damage detection.

2 State of the art

An established approach for condition monitoring of gear boxes is to measure vibration and an associated method is to measure acoustic emissions. Furthermore, the temperature

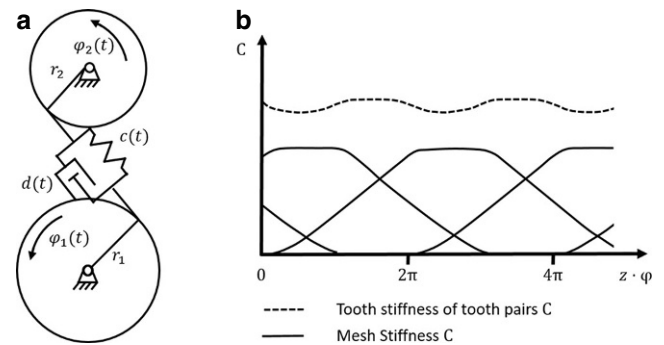


Fig. 1 a Modelling of gear meshing (cf [11]), b stiffness of gear meshing over multiple teeth for helical gears (cf [13])

may be measured or wear debris monitored [6, 7]. However, new approaches such as IAS are gaining in popularity [4, 5, 8]. Compared to the vibration measurement on the gear box housing, the IAS signal is less disturbed by transfer path effects [9] and the speed information can be used for an order analysis [10].

2.1 Loaded transmission error

The meshing of two gears can be described as spring and damper with variable stiffness (see Fig. 1). Since the number of force-transmitting teeth changes periodically, the coupling stiffness also changes [11]. This results in angular and speed fluctuations called transmission error (TE). Besides the described tooth deflection, which is load-dependent, the TE has a non-load-dependent component caused by geometric deviations from the ideal profile [6, 8]. The resulting speed fluctuations can be measured as variations in the IAS and a structure-borne noise excitation that can be monitored by vibration sensors [4, 12]. In an undamaged state the gear meshing frequency can be observed. Damages such as pitting or cracks reduce the mesh stiffness and cause additional speed fluctuations [4, 12]. This causes an amplitude and phase modulation that can be observed in the frequency spectrum as sidebands around the gear mesh frequency [6].

2.2 Instantaneous angular speed

The IAS ω is the angular displacement $\Delta\varphi$ of the gear wheel divided by the corresponding time duration Δt [5]:

$$\omega = \frac{\Delta\varphi}{\Delta t} \quad (1)$$

The most common IAS measurement is carried out with optical encoders [10] and is calculated by measuring the elapsed time between uniformly spaced pulses using a clock frequency. A pulse generator produces these pulses per defined angular distance [5].

There are several applications to detect gear damage using IAS. Roy et al. [14] analysed the gear mesh frequency and surrounding sidebands to detect different gear damages. Coats et al. [15] describe a method to reduce speed fluctuations by order-tracking. Thus, IAS can be used for the extraction of time and frequency domain features to classify gear faults at varying torque and speed conditions [16].

Other applications use two optical encoders to calculate the transmission error, which can be used to measure wear depth [17] or to calculate the IAS difference to reduce external interference [10].

2.3 Magneto-resistive sensors

The magneto-resistive effect describes the change in electrical resistance of a material under the influence of a magnetic field [18]. This effect is often applied to the measurement of angular or linear movement. Typically a magneto-resistive sensor measures the movement of a dipole or multipole magnetic scale or alternatively of a gear wheel where the magnetic field is generated by a bias magnet [18, 19].

3 Method

In this section, first the test bench and test design and then the integration of the different MR sensor concepts into the gearbox are described.

3.1 Test bench

To measure IAS with MR-Sensors in this paper, a gearbox test bench at the Institute of Product Development and Machine Elements is used. Fig. 2 shows the Test bench and the National Instruments data acquisition chassis including modules.

The Test bench consists of two 1-stage gearboxes (SEW RX77/AD4). For measuring IAS, the MR sensors shown in Fig. 3 are integrated into the modified gearbox, acceleration sensors are mounted on the gearbox housing and a temperature sensor measures the oil temperature. The second gearbox serves as a backward transformer, the modified gearbox has an effective transmission ratio of $i_{mod} = -\frac{21}{51}$ and the second one has an effective transmission ratio of $i_{unmod} = -\frac{78}{24}$. The electric motors are 30kW asynchronous motors.

Fig. 2 Experimental Test bench

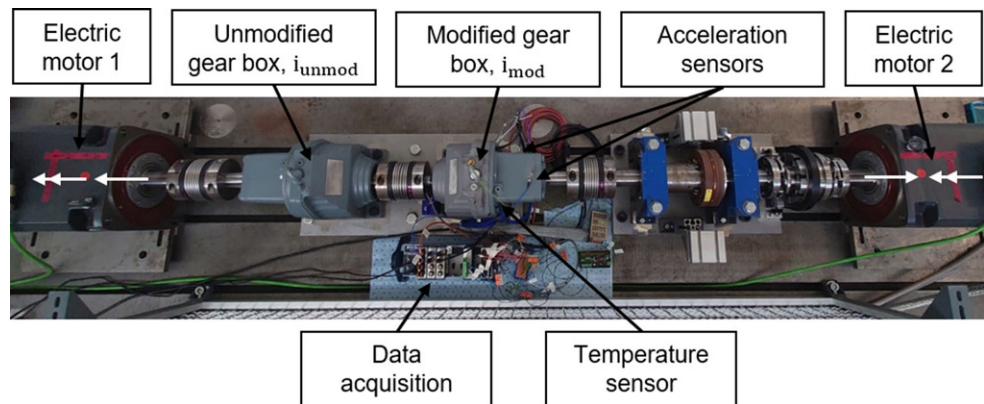
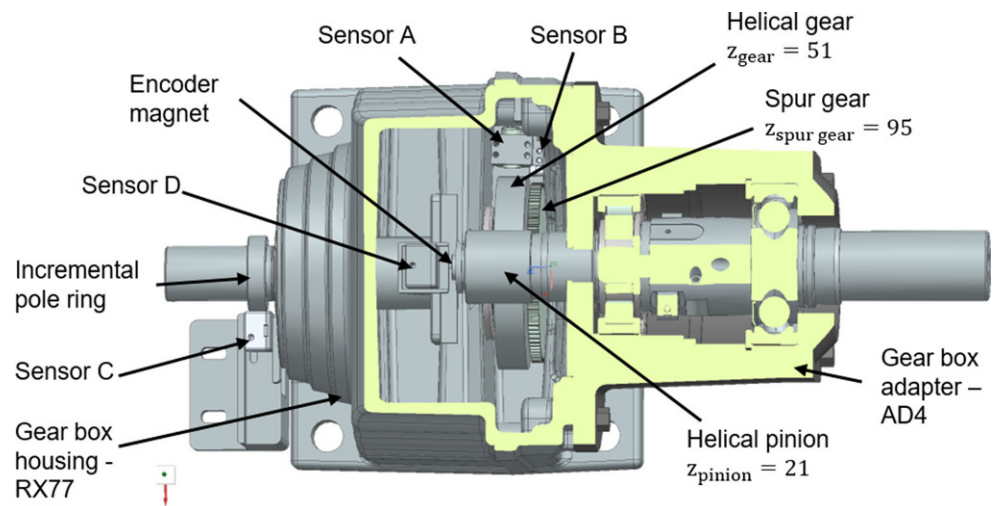


Fig. 3 Modified gear with integrated MR sensors



The signals are recorded using a National Instruments data acquisition system with the corresponding modules. It synchronizes the measurement and serves as a base clock for the counter measurement.

3.2 Test design

The experiments are operated in four quadrants. Electric motor 1 is speed-controlled and electric motor 2 is torque-controlled. Speed and torque direction are defined as shown in Fig. 2. The speed varies from $300 \frac{1}{\text{min}}$ to $2000 \frac{1}{\text{min}}$ and the torque starts at 0 Nm up to 96 Nm, both non-equidistantly distributed. The speed is measured and set at electric motor 1. The damage is artificially milled with a cylindrical-shaped diamond cutter onto the tooth flank of the pinion wheel. The first three damage levels simulate pitting, as round pits are milled with the diamond cutter tip into the tooth flank, starting with one tooth and expanding to three teeth. Afterward, the whole tooth flank is damaged using the diamond cutter cylindrical face. At each damage level, the before mentioned speed and torque parameters are varied.

3.3 Modifications of the gearbox

To integrate the MR sensors, the gearbox is modified. The sensors integrated are shown in Fig. 3. One spur gear with straight teeth is mounted onto the RX77 shaft as a measuring scale of Sensor B. Sensor A and Sensor B are fixed to the housing with an aluminum bracket. The sensing gap is

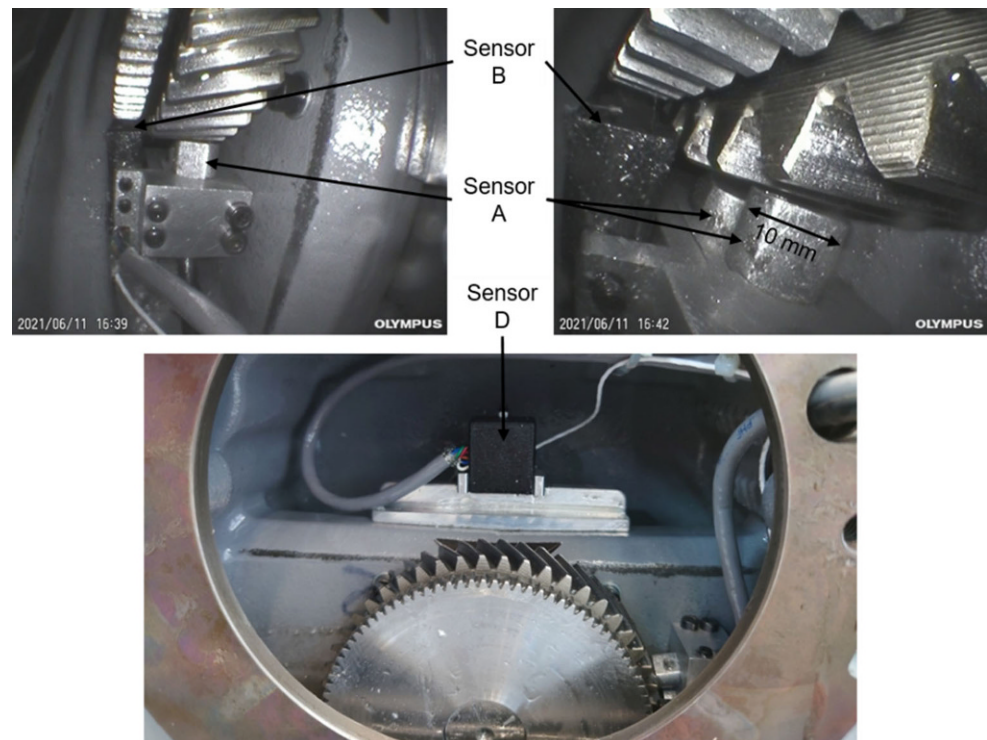
set by adjusting the sensors and calibrating the analog sensor signal. The measuring scale for Sensor D is an encoder magnet. The encoder magnet is centrally glued to the front side of the AD4 shaft. The measuring scale of Sensor C is an incremental pole ring glued onto the RX77 shaft outside of the housing.

3.4 Measuring concepts

To evaluate the feasibility of magnetoresistive sensors within the given scope, four different sensor concepts were selected for integration. All sensors are based on the same principle and are composed of two Wheatstone bridges. The raw output signals depend on the angle between sensor and magnetic field direction with a 90° phase shift and are sinusoidal-like oscillations. The following information was extracted from the respective datasheets and product information.

Sensor A is an anisotropic magnetoresistive (AMR) position sensor designed for highly dynamic non-contact measuring of the rotational speed of a ferromagnetic toothed wheel with high flexibility regarding permissible tooth pitches and also regarding the air gap between sensor and gear. The sensor itself consists of a sensor head with a magnetoresistive element and bias magnet plus a remote processing unit. Both units are accommodated in solid sealed aluminum housings. Sensor B contains a giant magnetoresistive (GMR) tooth sensor combined with a bias magnet and a high-resolution 9-bit interpolation-IC. The

Fig. 4 Implementation of MR sensors using the gear as measuring scale



Sensor B module is designed for several tooth structures with a 1 mm pitch. Sensor C is an AMR position sensor. The MR strips of this sensor are geometrically matched to a pole length of 0.5 mm (equal to a magnetic period of 1 mm). Sensor D is a position sensor based on the tunnel magnetoresistive (TMR) effect. As one electric period corresponds to one magnetic period, the sensor is capable of absolute angle measurement over 360° for example at the end of a motor shaft.

In this contribution the output of the MR sensors are two sinusoidal-like signals with a 90° phase shift for each tooth or pole. The angle φ is calculated using the atan2-function [20]. The angle calculated in this way is processed by unwrapping and scaling with the number of teeth or poles to obtain the correct angle for one revolution. Finally, the IAS is calculated with Eq. 1.

This contribution aims to evaluate the resolution and measurement accuracy of IAS measuring concepts with MR sensors to detect gear damages. The measuring scale of Sensor A is the standard helical gear of the RX77 (see Fig. 4). The installation space between helical gear and housing is used to integrate Sensor A. Thus, this sensor concept doesn't influence the functionality of the gearbox and no change in the basic function is required. Sensor A generates one sinusoidal signal per gear tooth, so the accuracy is limited and the speed direction cannot be measured using one sensor. Therefore, a second sensor with an offset of $1\frac{3}{4}$ teeth was integrated so that the phase shift between the two sensors is n times $360^\circ \pm 90^\circ$.

Due to the 51 teeth of the helical gear, the resolution is less compared to Sensor B (95 teeth) and Sensor C (256 poles). The measuring scale of Sensor B is not correctly aligned and shows an axial movement of 1.5 mm, caused by imperfections during the assembly. This results in a deviation of the sensing gap and poor signals of Sensor B.

Due to the resulting measurement errors, Sensor B is not further considered in this contribution.

A high-resolution sensor concept on the RX77 shaft is the incremental pole ring with 256 poles. This pole ring is the measuring scale of Sensor C, which integrated pulse generator generates 2^{13} pulses per revolution. The pole ring is additionally attached to the shaft outside of the housing (see Fig. 3). On the AD4 shaft, the absolute position is measured with an encoder magnet at the front side by Sensor D. The pulse generator generates 2^{12} pulses per revolution. To validate the damage detection with the described MR sensor concepts, acceleration sensors are mounted onto the housing of the AD4 (see Fig. 2), one is on the top and the other one on the side of the housing. The PT1000 temperature sensor measures the oil temperature of the modified gear. The test data was published by Koch et al. 2021 [21].

4 Results and discussion

In this section the MR sensor concepts described in chapter 3 are evaluated in regard to the detection of tooth flank damage. First, Sensor A in respect to the gear wheel as measuring scale is analysed. Second, damaged and undamaged data are examined in the frequency domain to evaluate the sensor concepts A, C and D as well as the acceleration sensor regarding the detection of the artificial tooth flank damage. Further data pre-processing is not applied.

4.1 Evaluation of helical gear as measuring scale

Sensor A generates one analog sinusoidal-like wave signal per tooth for each of the two sensors used in this concept. It is sensitive to variations to the orientation of the magnetic field, which is created by a permanent magnet and influenced by the teeth of the gear wheel. To evaluate the

Fig. 5 Peaks for five turns plotted over one turn of the Sensor A at $700\frac{1}{\text{min}}$ and 35 Nm

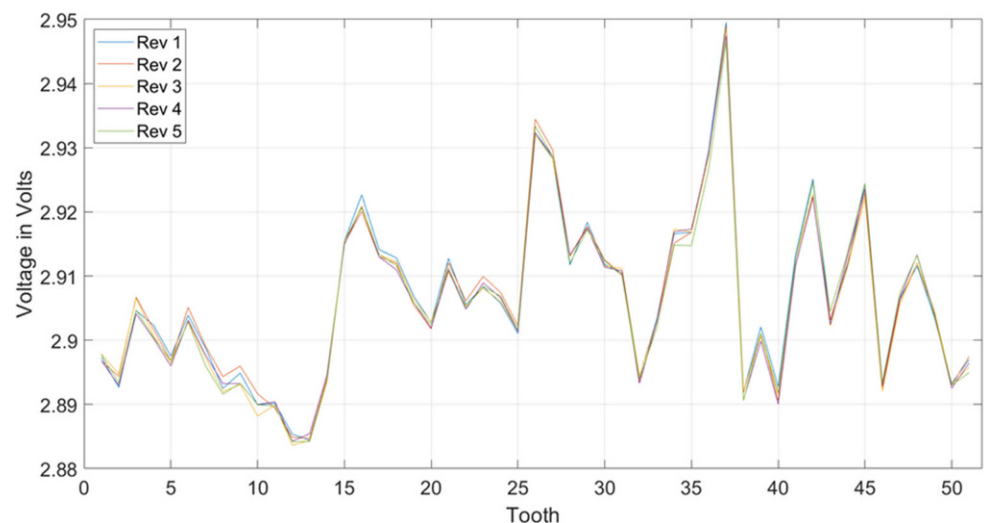
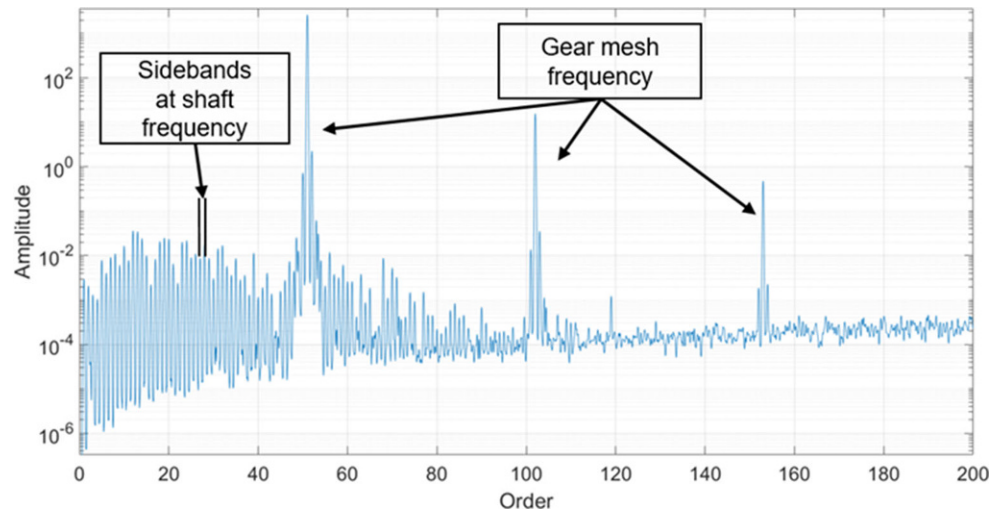


Fig. 6 Spectrum analysis of Sensor A at $2000 \frac{1}{\text{min}}$ and 70 Nm normalised with f_{RX77}



influence of the teeth of the gear wheel, the amplitude of every tooth is analysed. In Fig. 5 the highest peak of the sinusoidal-like oscillation of one revolution is plotted against the number of teeth. Five revolutions are considered to evaluate repeatability. Each tooth has a specific peak voltage, which is highly repeatable over multiple revolutions. This variation can be caused by varying working distances and geometrical arrangements due to manufacturing and assembly deviations of the gear wheel and the orientation of the sensor in respect to the gear wheel.

In the following, the order spectrum of the IAS is analysed. First, the gear mesh frequency (GMF) is calculated using the shaft speed of the AD4 adapter ($n_{AD4} = 2000 \frac{1}{\text{min}}$) and the number of teeth of the pinion ($z_{\text{pinion}} = 21$):

$$\text{GMF} = \frac{n_{AD4}}{60 \frac{\text{s}}{\text{min}}} \cdot z_{\text{pinion}} = 700 \text{ Hz} \quad (2)$$

The order is calculated using the shaft frequency, which connects the two gearboxes f_{RX77} . It is calculated using the GMF and the number of teeth of the gear ($z_{\text{gear}} = 51$):

$$f_{RX77} = \frac{\text{GMF}}{z_{\text{gear}}} = 13.7 \text{ Hz} \quad (3)$$

So, the GMF is located at the 51st order and the sidebands are one apart in the order spectrum normalised with f_{RX77} (see Fig. 6).

The gear mesh frequency and higher orders of the modified gear are identifiable in the order spectrum of Sensor A (see Fig. 6). Sidebands at the distance of the rotational frequency superimpose the signal over the whole frequency range. This is caused by the signal deviation of every tooth per revolution, as shown in Fig. 5, causing a strong sideband effect similar to a distributed damage [6].

4.2 Tooth flank damage detection with MR sensors

Damage detection of involute gear trains can be carried out with an order and sideband analysis [6]. The damage of the tooth flank is artificially milled onto the tooth flank as described in Chapter 3. For the following evaluation, one entire tooth flank is damaged and two adjacent tooth flanks have artificial pitting, as shown in Fig. 7. The aim of the artificial damage is to provide first evidence that tooth flank damage can be detected by measuring IAS with the presented MR sensor concepts. Furthermore, the manual milling process is not precise and the gear meshing contact zone is not exactly known. Therefore, in this contribution, large damages are milled onto the tooth flank, which certainly influences the meshing of the gears.

The first order gear mesh frequency (51st order in the spectrum in Fig. 8) and the first five sidebands are analysed at $2000 \frac{1}{\text{min}}$ and 70 Nm. Increasing Sidebands with the frequency of the pinion wheel shaft are expected around the gear mesh frequency due to the artificial tooth flank dam-

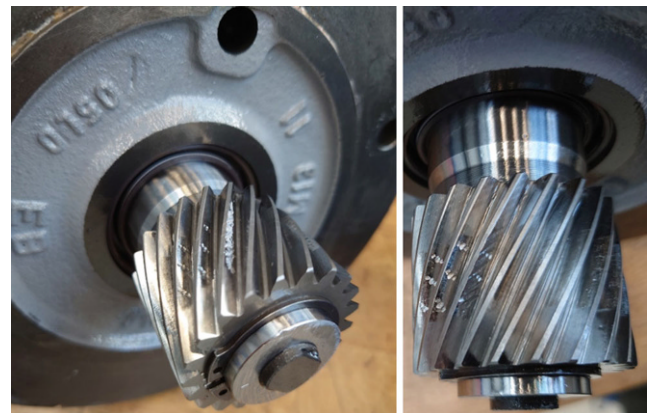
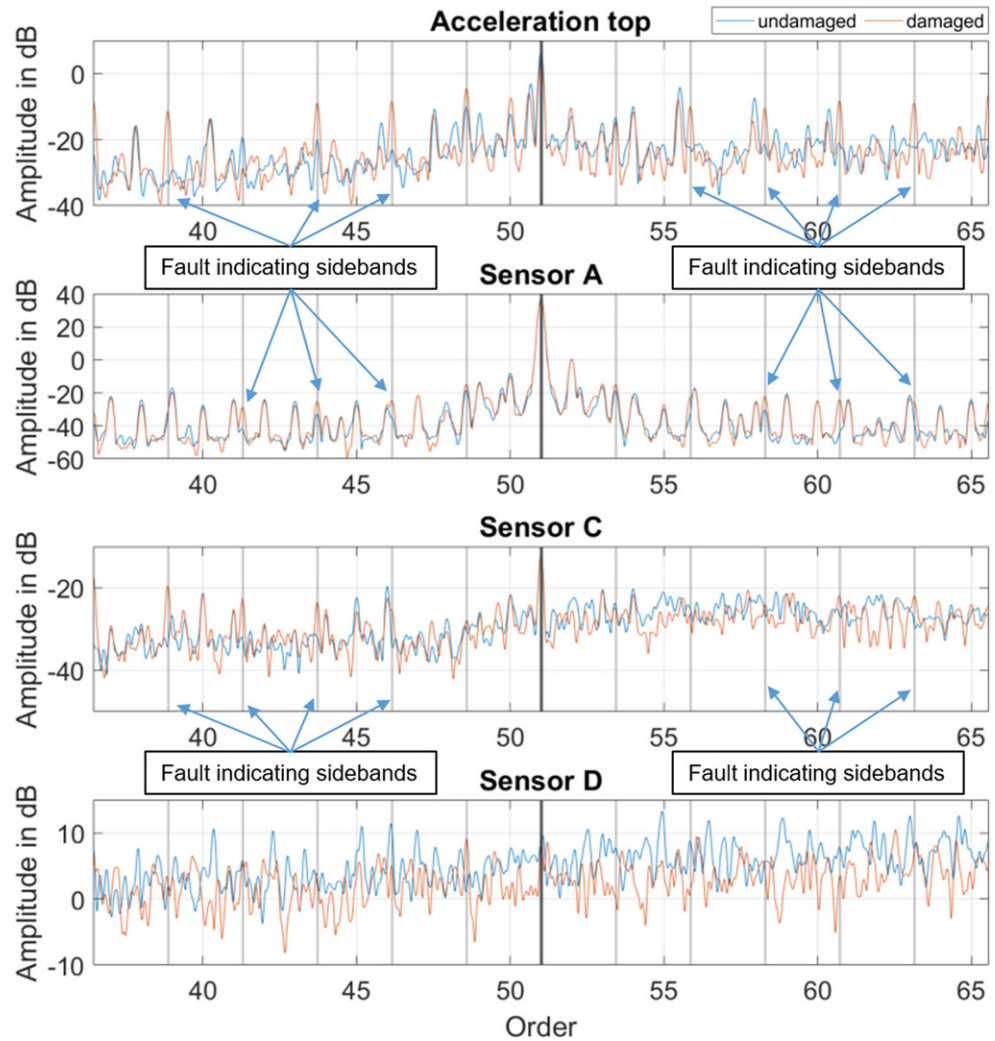


Fig. 7 Artificially milled tooth flank damage and pitting's on the pinion wheel

Fig. 8 Undamaged and damaged spectrum of the sensor concepts at $2000 \frac{1}{\text{min}}$ and 70 Nm



age. In Fig. 8 the spectrum analysis of the damaged and undamaged state is shown, the gear mesh frequency and the sidebands are displayed by vertical lines.

In the spectrum of the acceleration sensor and the IAS spectrum of Sensor C, sidebands in the frequency spectrum of the damaged pinion wheel shaft are significantly increased, especially the sidebands of orders three to six. The IAS spectrum of Sensor C also shows distinct sidebands with the rotation frequency of the gear wheel shaft. For the IAS spectrum of Sensor A, the sidebands in the frequency spectrum of the damaged pinion are also elevated compared to the undamaged state, but not as significantly as in the previously described spectra. This is due to the

high sideband amplitudes that occur even in the undamaged state, as shown in Fig. 6. Because the gear wheel is used as a measuring scale and the manufacturing and assembly deviations cause amplitude and phase modulation. The IAS spectrum of Sensor D shows little change of sidebands in the spectrum, but no clear rise of sidebands in the damaged compared to the undamaged state can be observed. However, further investigations are necessary to evaluate if this observation is caused by the damage or other influencing factors.

In addition to this visual analysis of the spectrum, the increase of the GMF and surrounding five sidebands are calculated by dividing the amplitude of the damaged by

Table 1 Amplitude quotient value of damaged by undamaged of the GMF and five surrounding sidebands

	-5	-4	-3	-2	-1	GMF	+1	+2	+3	+4	+5
Acceleration	75	0.1	14	36	4	0.6	0.5	12	7	11	37
Sensor A	0.7	26	6	7	2	1	2	2	6	74	3
Sensor C	14	7	5	2	1	1	0.6	0.8	0.8	3	3
Sensor D	2	1	0.6	0.5	3	0.7	0.2	0.2	0.5	0.5	0.6

the undamaged state. The change of this quotient value is shown in Table 1 rounded to one significant digit. Significant increases can be seen for the acceleration sensor, Sensor A and C, but there are also decreasing amplitudes in the damaged state. However, the increase is much higher than the decrease, which indicates the damage. Nevertheless, this has to be further investigated to clearly state that tooth flank damage can be detected.

4.3 Discussion

Summing up the analysis, it can be stated that tooth flank damage influences the first gear mesh frequency and the surrounding five sidebands. This change can be detected with the integrated MR sensors A and C. The MR sensor concept A has a high phase and amplitude modulation due to manufacturing deviations of the gear wheel and possible assembly deviations of the gearbox as well as the sensor in respect to the gear wheel, which superimposes the phase and amplitude modulation caused by tooth flank damage. Comparing the MR sensor concepts with the acceleration sensor, the amplitude of the sidebands increases less. The main cause could be the described amplitude and phase modulation due to manufacturing and assembly deviations. For an order analysis, however, the sensor concept using an acceleration sensor additionally needs the speed information. This information is inherent in the IAS signal so that no further sensors or information are needed for an order analysis.

An excerpt of the test data is discussed in this contribution [21], further evaluations should be carried out to gain more confidence in the results presented.

5 Conclusion

In this contribution, four different sensor concepts using MR sensors to measure IAS in a one-stage gearbox are presented, which have little (Sensor C and D) to no influence (Sensor A and B) on the power transmitting elements. To evaluate the detection of tooth flank damage with these concepts, tests were carried out with artificial damage milled onto the tooth flank. The results were compared to an acceleration sensor and evaluated by an order analysis of the first gear mesh frequency and the surrounding sidebands.

The evaluation of the MR sensor concepts has shown that the presented MR sensor concepts A and C can detect tooth flank damages of helical gears. Using the gear wheel as a measuring scale the tooth-specific deviation has a significant influence on the signal, which raises two questions: Can this be used for a tooth-specific evaluation or can this effect be reduced by pre-processing of the sensor data?

The MR sensor concepts have been evaluated on artificial damages, it still needs to be verified that real and less severe damages can also be detected.

This study does not yet take the information of the absolute position into account to extract information, which can also enhance the damage detection possibilities. Furthermore, the spectrum of the raw IAS data was evaluated, no pre-processing was carried out, which could improve the detection of gear damage even in the case of minor damage. As the speed information is inherent in the IAS signal a speed-independent damage detection is possible.

Furthermore, there is still a need to optimize the integration process, as the manufacturing and assembly deviations significantly influence the acquired signal, or reduce this influence by pre-processing of the raw signal.

Acknowledgements The support of this project through the SEW-EURODRIVE GmbH & Co KG and the European Regional Development Fund (ERDF) is gratefully acknowledged.

Funding Open Access funding enabled and organized by Projekt DEAL.

Open Access This article is licensed under a Creative Commons Attribution 4.0 International License, which permits use, sharing, adaptation, distribution and reproduction in any medium or format, as long as you give appropriate credit to the original author(s) and the source, provide a link to the Creative Commons licence, and indicate if changes were made. The images or other third party material in this article are included in the article's Creative Commons licence, unless indicated otherwise in a credit line to the material. If material is not included in the article's Creative Commons licence and your intended use is not permitted by statutory regulation or exceeds the permitted use, you will need to obtain permission directly from the copyright holder. To view a copy of this licence, visit <http://creativecommons.org/licenses/by/4.0/>.

References

1. Kirchner E (2020) Werkzeuge und Methoden der Produktentwicklung. Von der Idee zum erfolgreichen Produkt. Springer Vieweg, Berlin
2. Bechev D, Sauer B, Kösch P, Herder CF, Aurich JC, Wiegel T, Seewig J (2017) Strategy for the diagnosis and prediction of machine failures for developing availability-oriented business models in capital goods. *Int Sci J* 2:86–90
3. Slatter R (2018) Robust Magnetic Sensors for Availability-oriented Product-Service Systems. *Proc. of Smart Systems Integration Conference, Dresden*
4. Liang L, Liu F, Kong X, Li M, Xu G (2019) Application of instantaneous rotational speed to detect gearbox faults based on double encoders. *Chin J Mech Eng* 32:1. <https://doi.org/10.1186/s10033-019-0324-z>
5. Li Y, Gu F, Harris G, Ball A, Bennett N, Travis K (2005) The measurement of instantaneous angular speed. *Mech Syst Signal Process* 19:786–805. <https://doi.org/10.1016/j.ymssp.2004.04.003>
6. Randall RB (2011) Vibration-based condition monitoring. Industrial, aerospace, and automotive applications. Wiley, Chichester, Hoboken. <https://doi.org/10.1002/9780470977668>

7. Collacott RA (1977) *Mechanical Fault Diagnosis and condition monitoring*. Springer, Dordrecht <https://doi.org/10.1007/978-94-009-5723-7>
8. Remond D (1998) Practical performances of high-speed measurement of gear transmission error or torsional vibrations with optical encoders. *Meas Sci Technol* 9:347–353. <https://doi.org/10.1088/0957-0233/9/3/006>
9. Martin G, Vogel S, Schirra T, Vorwerk-Handing G, Kirchner E (2018) Methodical evaluation of sensor positions for condition monitoring of gears. In: Ekströmer, Schütte (eds) 2018—DS 91: Proceedings of NordDesign
10. Liang L, Lei Z, Li M, Kong X (2018) Feature extraction of gearbox based on order analysis of instantaneous angular speed. In: Sun M, Zhang H (eds) *IEEE 7th Data Driven Control and Learning Systems Conference (DDCLS'18)*. IEEE, Piscataway. <https://doi.org/10.1109/DDCLS.2018.8516049>
11. Tamminana VK, Kahraman A, Vijayakar S (2007) A study of the relationship between the dynamic factors and the dynamic transmission error of spur gear pairs. *J Mech Des* 129:75–84. <https://doi.org/10.1115/1.2359470>
12. Li B, Zhang X, Wu J (2017) New procedure for gear fault detection and diagnosis using instantaneous angular speed. *Mech Syst Signal Process* 85:415–428. <https://doi.org/10.1016/j.ymssp.2016.08.036>
13. Schlecht B (2010) *Maschinenelemente 2: Getriebe, Verzahnungen und Lagerungen*. Pearson
14. Roy SK, Mohanty AR, Kumar CS (2016) Fault detection in a multi-stage gearbox by time synchronous averaging of the instantaneous angular speed. *J Vib Control* 22(2):468–480. <https://doi.org/10.1177/1077546314533582>
15. Coats MD, Randall RB (2014) Single and multi-stage phase demodulation based order-tracking. *Mech Syst Signal Process* 44(1–2):86–117. <https://doi.org/10.1016/j.ymssp.2013.09.016>
16. Fedala S, Rémond D, Felkaoui A, Selmani H (2019) Intelligent gear fault diagnosis in normal and non-stationary conditions based on instantaneous angular speed, differential evolution and multi-class support vector machine. Springer, Cham, pp 16–33. https://doi.org/10.1007/978-3-319-96181-1_2
17. Chin ZY, Smith WA, Borghesani P, Randall RB, Peng Z (2021) Absolute transmission error: a simple new tool for assessing gear wear. *Mech Syst Signal Process* 146:107070. <https://doi.org/10.1016/j.ymssp.2020.107070>
18. Slatter R (2018) Low power miniaturized tunnel magnetoresistive (TMR) sensors for Industry 4.0 applications. *GMM-Fachbericht 92: Mikro-Nano-Integration, Dortmund*
19. Slatter R (2019) Condition monitoring of gearboxes using magnetoresistive sensors. *International Conference on Gears 3*, pp 229–244
20. de Dinechin F, Istoan M (2015) Hardware implementations of fixed-point Atan2. 2015 *IEEE 22nd Symposium on Computer Arithmetic*. IEEE, pp 34–41 <https://doi.org/10.1109/ARITH34996.2015>
21. (2021) Measurement of Instantaneous Angular Speed in a Helical Gear Box using Magnetoresistive Sensors, Koch, Y., Martin, G., Kirchner, E., Quirinheim Pais, D., Rauber, L., Lenze, T., Slatter, R. U Tu Darmstadt. <https://doi.org/10.48328/tudatalib-651>